J Physiol 595.15 (2017) pp 5285–5300

The Journal of Physiology

Presence of ethanol-sensitive glycine receptors in medium spiny neurons in the mouse nucleus accumbens

B. Förstera[1,*], B. Muñoz[1,*], M. K. Lobo[2], R. Chandra[2], D. M. Lovinger[3] and L. G. Aguayo[1]

[1] *Department of Physiology, University of Concepcion, Concepcion, Chile*
[2] *Department of Anatomy and Neurobiology, University of Maryland School of Medicine, 20 Penn Street, HSF II Rm 251, Baltimore, MD 21201, USA*
[3] *Laboratory for Integrative Neuroscience, National Institute on Alcohol Abuse and Alcoholism, National Institutes of Health, Bethesda, MD, USA*

Key points

- The nucleus accumbens (nAc) is involved in addiction-related behaviour caused by several drugs of abuse, including alcohol.
- Glycine receptors (GlyRs) are potentiated by ethanol and they have been implicated in the regulation of accumbal dopamine levels.
- We investigated the presence of GlyR subunits in nAc and their modulation by ethanol in medium spiny neurons (MSNs) of the mouse nAc.
- We found that the GlyR α1 subunit is preferentially expressed in nAc and is potentiated by ethanol.
- Our study shows that GlyR α1 in nAc is a new target for development of novel pharmacological tools for behavioural intervention in drug abuse.

Abstract Alcohol abuse causes major social, economic and health-related problems worldwide. Alcohol, like other drugs of abuse, increases levels of dopamine in the nucleus accumbens (nAc), facilitating behavioural reinforcement and substance abuse. Previous studies suggested that glycine receptors (GlyRs) are involved in the regulation of accumbal dopamine levels. Here, we investigated the presence of GlyRs in accumbal dopamine receptor medium spiny neurons (MSNs) of C57BL/6J mice, analysing mRNA expression levels and immunoreactivity of GlyR subunits, as well as ethanol sensitivity. We found that GlyR α1 subunits are expressed at higher levels than α2, α3 and β in the mouse nAc and were located preferentially in dopamine receptor 1 (DRD1)-positive MSNs. Interestingly, the glycine-evoked currents in dissociated DRD1-positive MSNs were potentiated by ethanol. Also, the potentiation of the GlyR-mediated tonic current by ethanol suggests that they modulate the excitability of DRD1-positive MSNs in nAc. This study should contribute to understanding the role of GlyR α1 in the reward system and might help to develop novel pharmacological therapies to treat alcoholism and other addiction-related and compulsive behaviours.

(Received 12 November 2016; accepted after revision 5 May 2017; first published online 19 May 2017)
Corresponding author L. G. Aguayo: Laboratory of Neurophysiology, Department of Physiology, University of Concepcion, Barrio Universitario S/N, PO Box 160-C, Concepcion, Chile. Email: laguayo@udec.cl

Abbreviations AP, action potential; BS, brainstem; ct, threshold cycle; DRD1, dopamine receptor D1; DRD2, dopamine receptor D2; D1+, DRD1-positive neurons; D1−, DRD1-negative neurons; GABA(A)R, type A GABA receptor; GlyR, glycine receptor; GlyT1, glycine transporter 1; HC, hippocampus; ICC, immunocytochemistry; IHC, immunohistochemistry; MSN, medium spiny neuron; nAc, nucleus accumbens; SC, spinal cord; STN, strychnine; VTA, ventral tegmental area.

*These authors contributed equally to the study.

DOI: 10.1113/JP273767

Introduction

The nucleus accumbens (nAc) is an important region of the mesolimbic system that is involved in addiction-related behaviours (Di Chiara, 2000; Spanagel, 2009). It sends and receives GABAergic projections to and from the ventral tegmental area (VTA), and also receives GABAergic and cholinergic projections from the lateral septum and glutamatergic inputs from the medial prefrontal cortex, amygdala, hippocampus (HC) and paraventricular nucleus. In addition, the nAc receives an important dopaminergic input from the VTA (Koob & Nestler, 1997; Koob, 1998; Meredith, 1999; Martin & Siggins, 2002; Jonsson *et al.* 2017). Interestingly, increased levels of dopamine in the nAc have been implicated in reward-seeking and drug-related behaviours. Furthermore, it was reported that ethanol increased dopamine levels in the nAc (Di Chiara, 2000; Volkow & Li, 2004).

Dopamine activates two distinct types of metabotropic receptors in the nAc, D1 and D2 type dopamine receptors (DRD1 and DRD2), which are expressed in distinct cell populations. The DRD1 is a component of the direct pathway from nAc to VTA and is believed to stimulate reward-seeking behaviour (Koob & Nestler, 1997). It is most likely that neuronal activity within the nAc can affect the flux of information in the mesolimbic pathway and therefore affect addiction-related behaviours. In this sense, synaptic and intrinsic excitability are fundamental to regulate the pathway output, and it is known that chronic alcohol exposure affects changes in the excitability of accumbal neurons (Jeanes *et al.* 2011; Renteria *et al.* 2017). The activity of DRD1-positive (D1+) medium spiny neurons (MSNs) is regulated by GABAergic, dopaminergic and glutamatergic inputs from several areas (Koob & Nestler, 1997; Koob, 1998; Martin & Siggins, 2002). On the other hand, a potential role of glycine receptors (GlyRs) on accumbal function has not been examined in detail.

GlyRs are widely expressed in the CNS, primarily in the spinal cord (SC) and brainstem (BS). Recently, GlyRs were also found in the cerebellum (Husson *et al.* 2014) and in supra-tentorial regions such as the cerebral cortex, HC and raphe nuclei (Eichler *et al.* 2009; Maguire *et al.* 2014; Salling & Harrison, 2014). Mesolimbic regions such as the VTA and the nAc were also reported to express GlyRs of a still unidentified molecular nature (Ye *et al.* 2001; Martin & Siggins, 2002; Molander *et al.* 2005; Lynch, 2009). This is of interest because the presence of GlyRs in these mesolimbic areas might be relevant for the rewarding properties of ethanol as they appear to regulate ethanol consumption, as well as the release of dopamine in the presence and absence of ethanol (Molander *et al.* 2005; Molander & Soderpalm, 2005*b*; Li *et al.* 2012). Furthermore, it was reported that Org25935, an inhibitor for the astrocytic glycine transporter 1 (GlyT1), affects ethanol consumption and the levels of dopamine in nAc (Molander *et al.* 2007). Therefore, the aim of this study was to elucidate the type of GlyR subunits expressed in accumbal MSNs and to examine if they are affected by ethanol. We employed conventional and quantitative real-time PCR, immunohisto- and cytochemistry, as well as electrophysiological recordings, to examine the hypothesis that accumbal D1+ MSNs express functional, ethanol-sensitive GlyRs that have a role on the excitability of these neurons.

Methods

Ethical approval

Animal care and experimental protocols for this study were approved by the Institutional Animal Care and Use Committee at the University of Concepción. Male C57BL/6J DRD1-GFP transgenic mice (1–4 months old) were housed and cared for as described below and killed by decapitation after anaesthesia with isoflurane as described. The use of animals complied with the laws, regulations and policies regarding humane care and use of laboratory animals in reference to the Chilean Policies on Human Care and Use of Laboratory Animals, and followed the guidelines for ethical protocols and care of experimental animals established by the National Institutes of Health (NIH, Bethesda, MD, USA).

Experimental animals

Male C57BL/6J mice were acquired from the Jackson Laboratory (Bar Harbor, ME, USA), and DRD1-GFP [Tg(Drd1a-EGFP)x60Gsat/Mmmh] transgenic mice with a C57BL/6J background were obtained from Dr David M. Lovinger (NIH) and maintained in house in a C57BL/6J background. Mice were individually housed in groups of 2–4 on a 12 h light/dark cycle and given food and water *ad libitum*. For preparation of sections, dissociated neurons, mRNA samples and immunohistochemistry (IHC), DRD1-GFP mice of postnatal age 90–110 days were used. For electrophysiology, 30-day-old mice were used. Animals were anaesthetized with isoflurane and killed by decapitation. The brain was quickly excised and placed in ice-cold cutting solution (see below) for further preparation. When possible, tissues from each animal were used for multiple experiments.

Conventional and real-time quantitative PCR

Tissue of nAc, HC, BS and SC from male DRD1-GFP mice was collected and preserved for a maximum of 10 days at −20°C in RNAlater (Ambion, UK) before

further processing. Total RNA was isolated from samples using the NucleoSpin RNA PLUS isolation kit (Macherey-Nagel, Düren, Germany) including genomic DNA elimination columns, followed by digestion with DNase I (Macherey-Nagel) for 30 min and NucleoSpin RNA clean-up to remove trace amounts of genomic DNA. cDNA was prepared from 0.5 μg of total RNA with the Affinity Script qPCR cDNA Synthesis Kit (Agilent Technologies, Santa Clara, CA, USA), including preparation of RNA sample-free negative controls (H_2O) and cDNA (reverse-transcriptase)-free negative controls. PCR on cDNA-free negative controls was performed in parallel to exclude amplification of genomic DNA. PCRs were run using 2 μl cDNA for 35 cycles with an annealing temperature of 56°C in a Mastercycler (Eppendorf, Hamburg, Germany) for conventional PCR ($n = 2$, not shown) and 40 cycles with an annealing temperature of 52°C in a Strategene Mx3005P cycler (Agilent Technologies) for real-time quantitative PCR (qPCR) ($n = 4$), using the Brilliant II Cybrgreen QPCR Master Mix (Agilent Technologies), including melting curves to control qPCR specificity. qPCR data were collected and analysed with MxPro (Agilent Technologies). GAPDH and β-actin were used as reference genes, and threshold cycles of GlyR expression were normalized to GAPDH due to lower variability between samples and runs. One qPCR run for GlyR β in nAc was excluded due to failed amplification as indicated by the absence of a sigmoid amplification curve and corresponding band in the control gel. The following primers were used for conventional and real-time qPCR: GlyR α1 forward 5′-CTGTTTGCCTGCTCTTCGTGT-3′ and reverse 5′-TGGGGAAACCGATGCGAGATA-3′; GlyR α2A forward 5′-ATCAACAGTTTTGGATCGGTCA-3′, GlyR α2B forward 5′-TCAACAGCTTTGGGTCAATAG-3′ and GlyR α2 reverse 5′-CCTTCAGCAACTTGTACT GG-3′; GlyR α3 forward 5′-TGGGTACACGATGAA TGATCTC-3′ and reverse 5′-TTAGCCCTGTCGATGAA GACC-3′; GlyR β forward 5′-TGAGCAAGCAGATGGG AAAGG-3′ and reverse 5′-TAACGTTGAAGAACAA GAAGCAG-3′ (Forstera *et al.* 2014). The following primers were used for real-time qPCR: GlyR α1 forward 5′-CTGTTTGCCTGCTCTTCGTGT-3′ and reverse 5′-T GGGGAAACCGATGCGAGATA-3′, GlyR α2 forward 5′-ATCAATGGGAAGGACATCAGGA-3′ and reverse 5′-G TTATCAGTGGTGACATCATGG-3′; GlyR α3 forward 5′-TGGGTACACGATGAATGATCTC-3′ and reverse 5′-TTAGCCCTGTCGATGAAGACC-3′; GlyR β forward 5′-ACGCAGCTAAGAAGAACACTGTGA-3′ and reverse 5′-CCAAGTTCCATTGTTGACTTCAATG-3′ (Kuhse *et al.* 1991; Froh *et al.* 2002); β-actin (Assey ID Rn.PT.39a.22214838.g; Integrated DNA Technologies, Inc., Coralville, IA, USA); GAPDH forward 5′-CCAGTAGACTCCACGACATAC-3′ and reverse 5′-AACCCATCACCATCTTCCAG-3′. The efficiency of all qPCR primers was determined by amplification ($n = 4$) of SC cDNA diluted 1:4, 1:16, 1:32 and 1:64 (Pfaffl, 2001).

Cell type-specific RNA isolation, cDNA synthesis and qPCR

Immunoprecipitation of polyribosomes was prepared from nAc of D1-Cre-RT and D2-Cre-RT mice according to a previous study (Chandra *et al.* 2015). In brief, four 14-gauge nAc punches per animal (four animals pooled per sample) were collected and homogenized by douncing in homogenization buffer and 800 μl of the supernatant was added directly to the HA coupled beads [100.03D (Invitrogen, Carlsbad, CA, USA); MMS-101R (Covance, Princeton, NJ, USA)] with constant rotation overnight at 4°C. The following day, magnetic beads were washed three times for 5 min in high salt buffer. Finally, RNA was extracted by adding TRK lysis buffer to the pellet provided in a MicroElute Total RNA Kit (Omega, GA, USA) according to the manufacturer's instructions. RNA was quantified with a NanoDrop (Thermo Scientific, Waltham, MA, USA). RNA was extracted using Trizol reagent (Invitrogen) and the Micro-Elute Total RNA Kit (Omega) with a DNase step (Qiagen, Hilden, Germany). All RNA quantity determinations were made on a Nanodrop. In total, 300–400 ng cDNA was then synthesized using a reverse transcriptase iScript cDNA synthesis kit (Bio-Rad, Hercules, CA, USA). mRNA expression changes were measured using qPCR with PerfeCTa SYBR Green FastMix (Quantabio, Beverly, MA, USA): input, $n = 4$; α1 and α2, $n = 5$; β, $n = 6$. Quantification of mRNA changes was performed using the $-\Delta\Delta$ CT method, using primers listed above and GAPDH as a housekeeping gene. GAPDH forward: AGGTCGGTGTGAACGGATTTG, GAPDH reverse: TGTAGACCATGTAGTTGAGGTCA.

IHC and immunocytochemistry (ICC)

IHC was performed as previously described (Stanic *et al.* 2010). Briefly, the whole brain of a 1-month-old male DRD1-GFP mouse was fixed at 4°C in Carnoy fixative overnight and embedded in paraffin. Frontal brain sections of 10 μm including the nAc (Fig. 1*A*–*C*) were prepared with an Autocut 2040 Microtome (Reichert-Jung, Germany) and mounted on poly-lysine-coated glass object slides (BNC, Germany) and de-paraffinated. Primary antibodies for IHC were incubated overnight and secondary antibodies were incubated for 3 h in Tris/HCl containing 1% BSA followed by three washes of 10 min in Tris/HCl, and mounted in Fluoromount mounting medium with 500 nM 4′,6-diamidino-2-phenylindole (DAPI). ICC was performed as described previously (Förstera *et al.* 2010). Briefly, dissociated neurons were prepared as described below and fixed for 15 min with paraformaldehyde (8%

in ice-cold PBS added to warm artificial cerebrospinal fluid (aCSF, final concentration 4%). The neurons were then washed three times with PBS and incubated for 15 min with 50 mM ammonium chloride in PBS followed by 4 min of permeabilization with 0.12% Triton-X in PBS containing 0.1% gelatin and subsequently washed twice with PBS/gelatin. Primary and secondary antibodies were incubated for 60 and 45 min in PBS/gelatin, respectively, followed by two washes with PBS/gelatin and two washes with PBS alone, and then finally mounted in Dako mounting solution (Dako North America, Inc., Carpinteria, CA, USA) containing 500 nM DAPI on glass object slides (BNC). All incubations were performed at room temperature unless otherwise noted. Green fluorescent protein (GFP) was visualized using a chicken anti-GFP antibody, producing a signal distribution comparable to the GFP signal in un-fixed sections of the nAc. GFP (1:50; chicken; Abcam, Cambridge, UK; Cat. No. AB13970), GlyR α (1:50; rabbit; Abcam; Cat. No. AB97628), GlyR α1 (1:50; mouse; mAb2b; Cat. No. 146111) and GlyR β (1:100; mouse; 299E7; Cat. No. 146211; Synaptic Systems, Göttingen, Germany) were combined with Cy3- and Alexa633-fluorescent labelled secondary antibodies (1:200; donkey; Jackson Laboratories, Inc., West Grove, PA, USA). All compounds and reagents were acquired from Merck (Darmstadt, Germany), Sigma-Aldrich (St Louis, MO, USA, USA) or Tocris (Bristol, UK), unless noted otherwise. Confocal images of a single optical section were acquired with 10×, 40× and 63× objectives in an LSM700 laser scanning microscope and ZEN software suit (Zeiss, Oberkochen, Germany) in the CMA core facility at the University of Concepción. ZEN (Zeiss) and Fiji ImageJ software (NIH) were used for image processing, and quantification and deconvolution of images was done with ZEN (Zeiss) and Fiji ImageJ software (NIH). Images of GlyR α1and GFP in dissociated neurons were taken from randomly chosen view-fields presenting multiple cells exhibiting different levels of GFP fluorescence. A maximum intensity projection for Fig. 5*A* and *B* was generated from a z-stack of 16 optical sections (7.23 μm total optical thickness). Quantification of GlyR α1 immunofluorescence of a single optical section at the centre of the cell soma in dissociated accumbal neurons was performed blind, before quantification of the GFP signal and grouping into D1+ and D1− cells. Cells with a high GFP signal were counted as D1+ ($28 \pm 3\%$, mean ± SEM, $n = 14$, Fig. 6*C*), while those with a low GFP signal were considered as D1− ($6 \pm 1\%$, mean ± SEM, $n = 19$, $^{***}P = 1.41 \times 10^{-9}$).

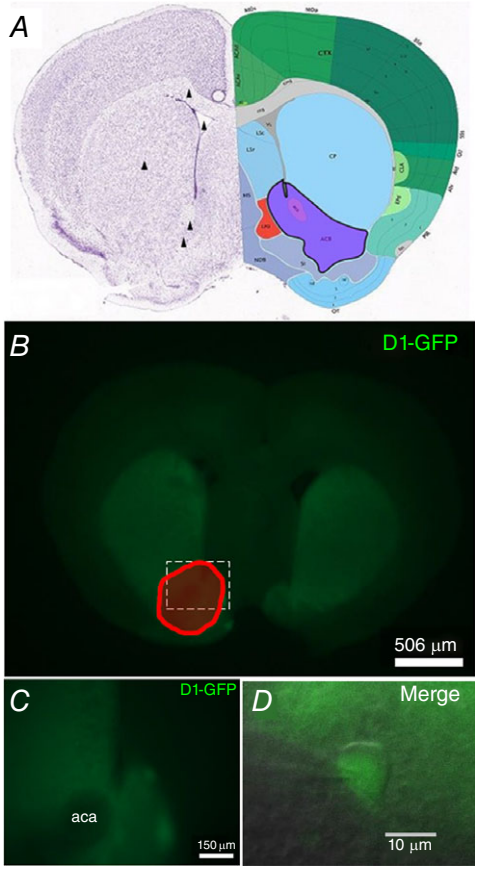

Figure 1. Coronal mouse brain slices of the nAc
A, coronal section from the adult mouse brain (Allan Brain Institute reference atlas) showing the nucleus accumbens (ACB, purple). Arrowheads indicate the anatomical landmarks used to prepare sections for nAc slice recordings and mechanical dissociation of nAc neurons (dorsal to ventral: corpus callosum, lateral ventricle, caudate putamen, anterior commissure and the nAc itself). *B*, photograph showing green fluorescence from D1-GFP neurons in a coronal brain section (300 μm). *C*, zoom of nAc surrounding the fascicle of the anterior commissure (aca). *D*, differential interference contrast infrared microscope image showing a merge of phase contrast and GFP fluorescence of patched D1+ MSNs in the nAc.

Preparation of brain slices

Frontal coronal slices containing the nAc were prepared immediately after excision and placement of the brain in ice-cold cutting solution (in mM: sucrose 194, NaCl 30, KCl 4.5, $MgCl_2$ 1, $NaHCO_3$ 26, NaH_2PO_4 1.2, glucose 10, saturated with 95% O_2 and 5% CO_2 and adjusted to pH 7.4). The brain was cut approximately 2 mm anterior to the cerebellum and the frontal part was glued with the cut surface to the chilled stage of a VT1200S vibratome (Leica, Wetzlar, Germany), and sliced to a thickness of 300–400 μm. Slices containing the nAc were transferred to aCSF solution (in mM: NaCl 124, KCl 4.5, $MgCl_2$ 1, $NaHCO_3$ 26, NaH_2PO_4 1.2, glucose 10, $CaCl_2$ 2, saturated with 95% O_2 and 5% CO_2 at 37°C for 1 h and adjusted to pH 7.4 and 310–320 mosmol l^{-1}). Brain slices were allowed to rest in O_2-perfused aCSF at 37°C for at least 1 h before recording or enzymatic treatment for dissociation.

Preparation of acutely dissociated neurons

Acutely dissociated neurons were prepared from acute brain slices. The nAc, including the core and shell region but not the fascicle of the anterior commissure, was dissected from acute brain slices and incubated for 30 min with 0.5 mg ml^{-1} pronase in oxygenated aCSF (95% O_2/5% CO_2, room temperature) at 37°C. Accumbal neurons were dissociated by mild mechanical trituration (10 times each with a 1000 μl and 200 μl micropipette and with a fire polished self-drawn glass-pipette) in trituration buffer [in mM: NaCl 20, *N*-methyl-D-glucamine (NMG) 130, KCl 2.5, $MgCl_2$ 1, Hepes 10, glucose 10, adjusted to pH 7.4 and 340 mosmol l^{-1}] and allowed to settle for 15–20 min before recording or fixation in oxygenated aCSF (95% O_2/5% CO_2, room temperature) on glass coverslips. Coverslips for ICC of dissociated neurons were previously coated with poly-lysine in PBS overnight and laminin in aCSF for 90 min at 37°C and washed three times with aCSF.

Electrophysiology

For electrophysiological recordings, acute brain slices were transferred to the recording chamber with aCSF solution saturated with 95% O2 and 5% CO_2 at room temperature. The slices were observed in a differential interference contrast infrared (DIC-IR) microscope using 10× and 40× objectives (Nikon Eclipse FN1, Tokyo, Japan) and perfused with oxygenated aCSF (95% O_2/5% CO_2, room temperature) at 2 ml min^{-1} and 30–32°C. Whole-cell current recordings of accumbal neurons were performed using the voltage-clamp technique. Patch pipettes with a resistance of 3–5 MΩ were prepared from filament-containing borosilicate micropipettes (World Precision Instruments, Sarasota, FL, USA) using a P-1000 micropipette puller (Sutter Instruments, Novato, CA, USA) and filled with internal solution (in mM: 120 KCl, 4.0 $MgCl_2$, 10 BAPTA, 0.5 Na_2-GTP and 2.0 Na_2-ATP, adjusted to pH 7.4 and 290–310 mosmol l^{-1}) or internal solution for current clamp recordings (in mM: 126

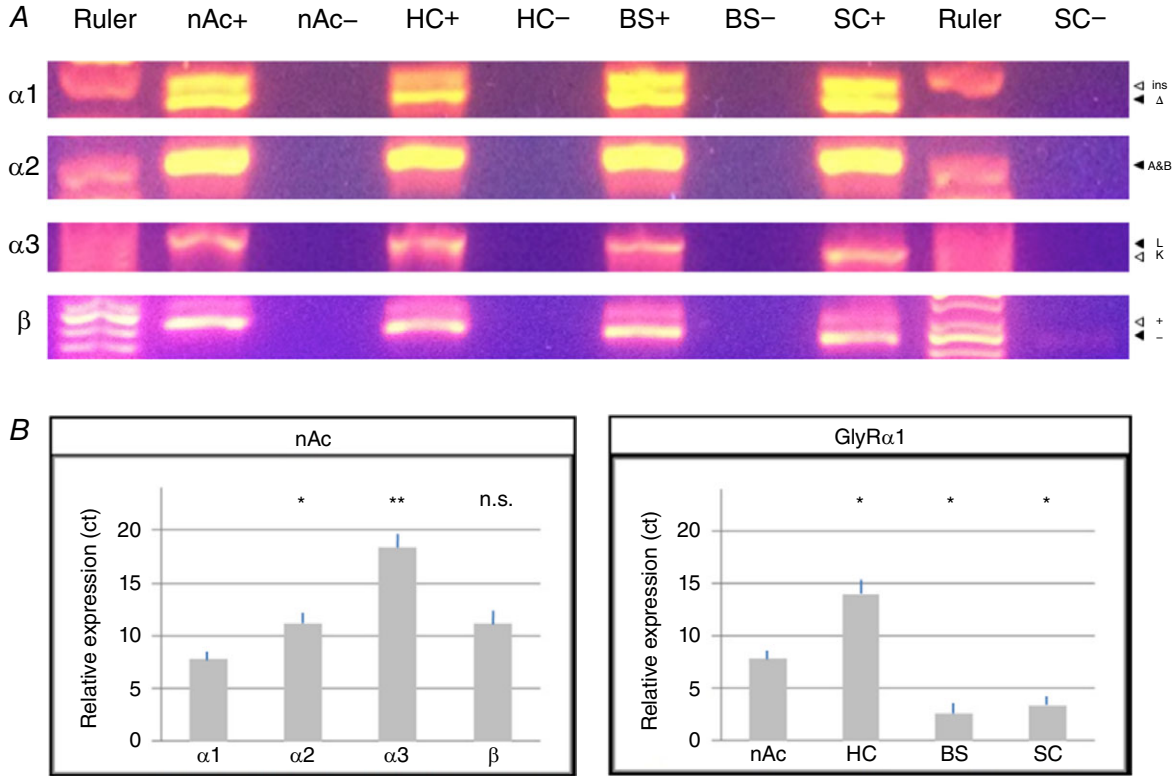

Figure 2. Conventional PCR and qPCR identify different GlyR subunits in the nAc
A, qPCR products confirm the finding of conventional PCR amplification of GlyR splice variants from nucleus accumbens (nAc), hippocampus (HC), brainstem (BS) and spinal cord (SC). Positive (+) and cDNA-free negative controls (–) showed that both splice variants of all tested GlyR subunits are expressed in nAc resulting in two distinct bands (α2A and β cannot be distinguished by size), although GlyR α3 expression is very low. GlyR α1**Δ**, α2A and α3L were more prevalent than their respective counterparts. *B*, quantitative real-time PCR of GlyR in nAc of DRD1/GFP mice indicates that α1 is the predominantly expressed subunit in nAc. Comparison of GlyR α1 expression in nAc, HC, BS and SC show that it was expressed at similar levels in BS and SC, but lower in nAc and HC. Threshold cycles (ct) were normalized to GAPDH and primer efficiency was accounted for (values are mean ± SEM; $n = 4$; Kruskal–Wallis and unpaired *post hoc* Bonferroni *t* test: $^{**}P < 0.01$, $^{*}P < 0.05$, n.s. not significant).

Table 1. qPCR for GlyR subunits in the nucleus accumbens (nAc), hippocampus (HC), brainstem (BS) and spinal cord (SC)

	GlyR α1	GlyR α2	GlyR α3	GlyR β
Ct value				
nAc	7.7 ± 0.4	11.1 ± 0.5	18.3 ± 0.7	11.1 ± 0.9
HC	14.0 ± 0.7	13.4 ± 0.6	20.5 ± 0.5	11.3 ± 1.0
BS	2.6 ± 0.5	11.9 ± 0.6	17.3 ± 0.4	9.6 ± 0.9
SC	3.4 ± 0.4	12.9 ± 0.2	16.6 ± 0.5	10.9 ± 0.9
P-value	GlyR α1	GlyR α2	GlyR α3	GlyR β
nAc *vs.* HC			n.s.	n.s.
	*0.025	*0.045	0.18	2.27
nAc *vs.* BS	*0.026	n.s.	n.s.	n.s.
	0.026	1.65	0.91	0.20
nAc *vs.* SC		n.s.	n.s.	n.s.
	*0.017	0.09	0.24	6.00
HC *vs.* BS				n.s.
HC *vs.* BS	***0.0002	*0.018	**0.002	0.050
HC *vs.* SC		n.s.		n.s.
	**0.002	1.15	***0.0003	1.16
BS *vs.* SC	n.s.	n.s.	n.s.	n.s.
	1.34	0.70	0.31	0.17
P-value	nAc	HC	BS	SC
α1 *vs.* α2	*0.021	n.s.	*** 0.0003	**0.0023
		1.83		
α1 *vs.* α3	**0.002	***0.0006	***0.00002	***0.0003
α1 *vs.* β	**0.002	**0.0017	**0.0025	*0.018
α2 *vs.* α3	n.s.	*0.031	**0.0024	*0.010
	0.17			
α2 *vs.* β	n.s.	n.s.0.29	n.s.	n.s.
	4.81		0.08	0.62
α3 *vs.* β	*0.031	**0.0030	**0.0035	**0.0066

Quantitative real-time PCR of GlyR in HC, BS and SC of DRD1/GFP mice. Threshold cycles were normalized to GAPDH and primer efficiency was accounted for (values are mean ± SEM; $n = 4$; Kruskal–Wallis and unpaired *post hoc* Bonferroni *t* test: ***$P < 0.01$, **$P < 0.01$, *$P < 0.05$, n.s. not significant).

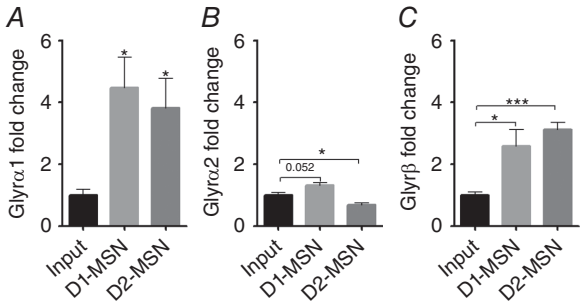

Figure 3. Expression of GlyR subunits in D1 and D2 MSNs
HA-tagged ribosomes were immunoprecipitated from nAc in D1-Cre-RiboTag and D2-Cre-RiboTag mice to obtain ribosome-associated mRNA from D1-MSNs and D2-MSNs. qPCR was performed using primers for GlyR α1 (*A*), GlyR α2 (*B*) and GlyR β (*C*) on MSN subtype ribosome-associated mRNA and input (non-immunoprecipitated) mRNA. α1 and β are enriched in both MSN subtypes relative to input, whereas GlyR α2 is enriched in D1-MSNs and reduced in D2-MSNs (values are mean ± SEM; $n = 4$–6 samples, 4 mice pooled per sample: ***$P < 0.001$, *$P < 0.05$ unpaired Student's *t* test).

potassium gluconate, 4 KCl, 10 Hepes, 10 BAPTA, 4 NaATP, 0.3 NaGTP, adjusted to pH 7.2 and 290 mosmol l^{-1}). Signals were captured using an Axopatch 200B amplifier (Axon Instruments, Union City, CA, USA) at a holding potential of −60 mV, displayed and stored on a personal computer using a 1322A Digidata device (Axon Instruments) and analysed with Clampfit 10.1 (Axon Instruments). The tonic current was measured at its baseline after 5 min application to the bath of a cocktail containing receptor blockers [bicuculline, 10 μM; 6-Cyano-7-nitroquinoxaline-2,3-dione (CNQX), 10 μM; D-(−)-2-amino-5-phosphonopentanoic acid (D-APV), 50 μM; TTX, 0.5 μM). The amplitude of the current was obtained by averaging all points recorded during a 2 min lapse. Under this condition, only a few synaptic currents associated with GlyRs (0.15 Hz) were recorded and they did not contribute to the averaged amplitude of the tonic response. All compounds and reagents were acquired from Merck or Sigma-Aldrich, unless noted otherwise.

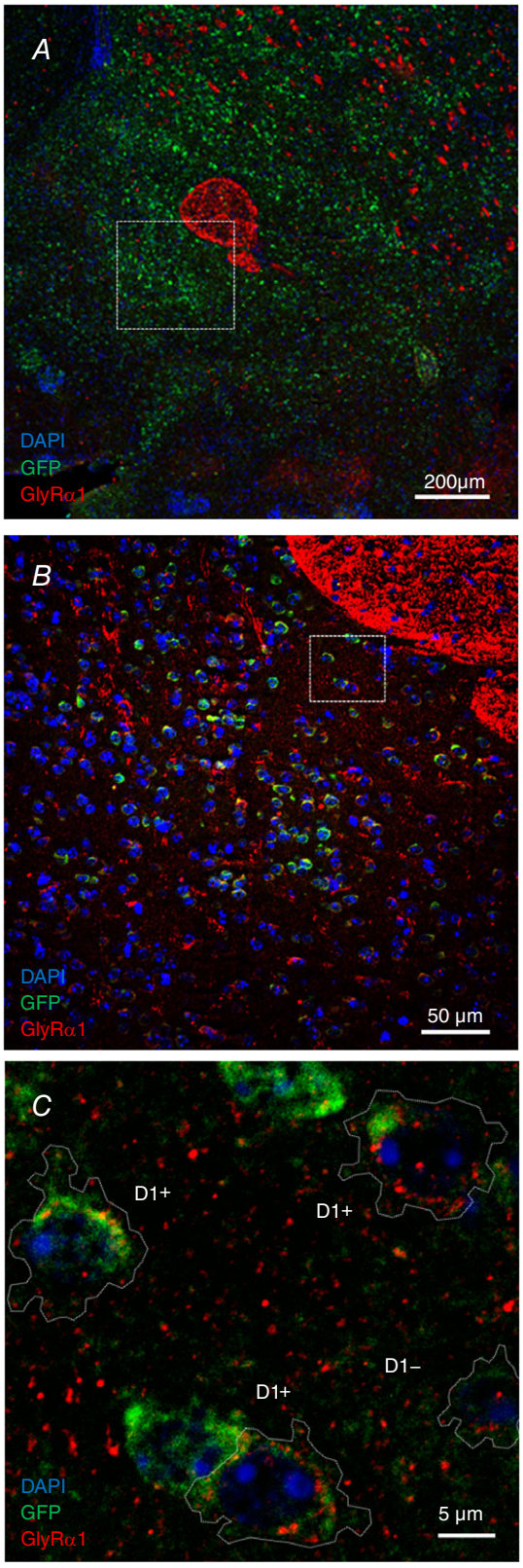

Figure 4. Immunohistochemistry shows the presence of GlyR α1 subunit in D1+ neurons in mouse brain sections of nAc
A, low magnification image of the nAc in a brain slice prepared from a GFP-DRD1 mouse with DAPI (blue), GFP (green) and GlyR α1 (red); white square indicates the region shown at higher magnification in *B*. *B*, higher magnification of the nAc core region. The α1 subunit was detected in cell bodies throughout the nAc; white square indicates the region shown at higher magnification in *C*. *C*, confocal optical section at highest magnification of the core region showing the presence of GlyR α1 clusters (red) in D1+ neurons and D1− cells (indicated by cell outline).

Statistical data analysis

Unpaired Student's *t* test was applied for statistical analysis unless otherwise noted. Kruskal–Wallis and unpaired *post hoc* Bonferroni *t* tests were used for analysis of region-specific real-time qPCR using VassarStats (Richard Lowry, Vassar College, Poughkeepsie, NY, USA). Slice recordings were analysed by one-way ANOVA using Origin 6 and 8 (Microcal, Inc., MA, USA). Quantified data are shown as mean ± SEM unless otherwise noted with the following: n.s., not significant; *, $P < 0.05$; **, $P < 0.01$; ***, $P < 0.001$.

Results

Presence of different messengers for GlyR subunits in nAc

Conventional and quantitative real-time PCR analysis was used to investigate the expression and relative predominance of GlyR subunits (α1, α2, α3 and β) in the nAc in comparison to HC, BS and SC (Fig. 2, Table 1). Conventional PCR amplification of GlyR splice variants revealed that both splice variants of all subunits were expressed in nAc, but the expression of GlyR α3 was comparatively lower. GlyR α1**Δ**, α2A and α3L were found to be more prevalent than their respective counterparts (Fig. 2*A*; GlyR α2A specific and α2B specific PCR not shown). Amplification of GlyR β also yielded two distinct bands and the results were confirmed by gel electrophoresis of qPCR products (Fig. 2*A*). These results indicate that nAc neurons express mostly GlyR α1 subunits.

To analyse the relative expression levels, quantitative real-time PCR of GlyR in nAc, HC, BS and SC was performed. We found that α1 was expressed at a moderately higher level (approximately 10-fold, $^{*}P = 0.022$) than α2 in nAc (Fig. 2*B*, Table 1), while BS and SC predominantly expressed α1, and in HC α1 and α2 were expressed at similar levels (Table 1). GlyR α2, α3 and β were expressed at similar levels in all tested brain regions with variations of less than 5-fold expression for α2 (HC *vs.* nAc $^{*}P < 0.05$) and β (n.s. $P = 0.41$), and less than 16-fold variation for α3. GlyR α1, however, was expressed at similarly strong levels in BS and SC, but approximately 30-fold less in nAc [threshold cycle (ct) 7.86 ± 0.72; nAc *vs.* HC, BS and SC $^{*}P < 0.05$) and approximately 2000-fold less in HC. Accordingly, conventional and quantitative

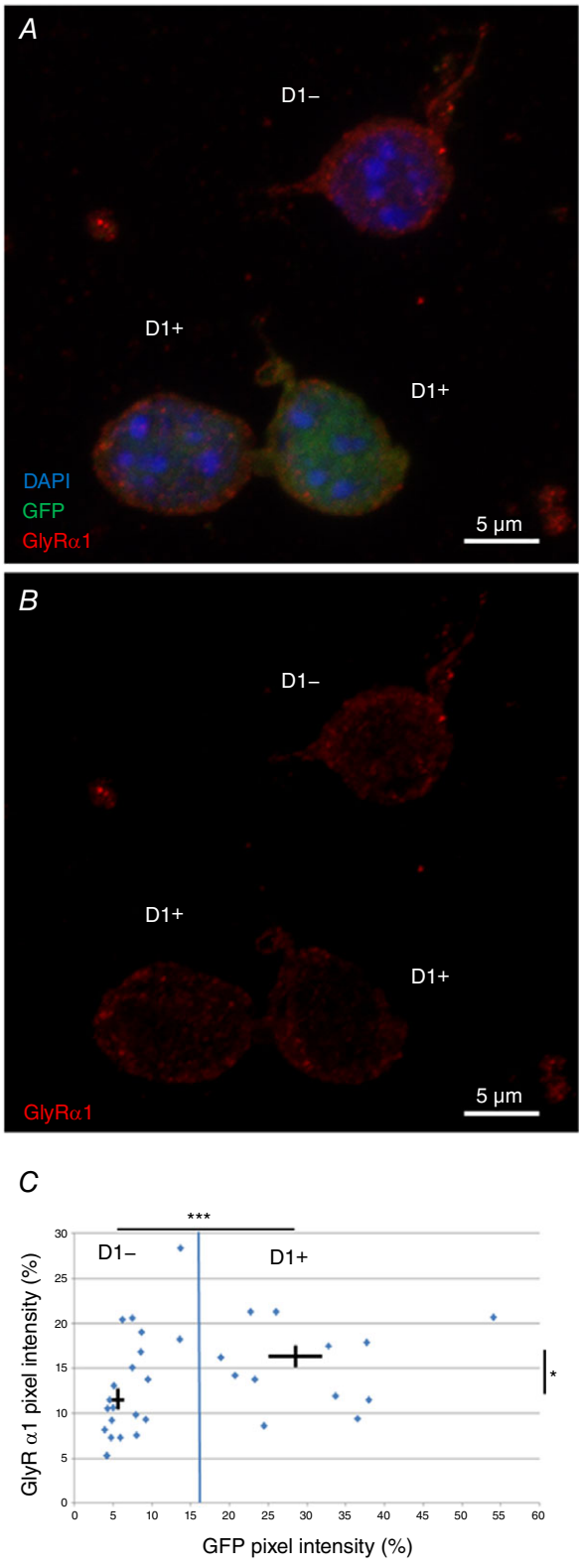

Figure 5. Immunocytochemistry showing GlyR α1 expression in acutely dissociated neurons from nAc
A, maximum intensity projection *z*-stack ($z = 16$; 7.23 μm) of acutely dissociated GFP-positive D1+ and negative D1− cells showing DAPI (blue), GFP (green) and GlyR α1 (red). *B*, maximum intensity projection of GlyR α1 (red) only in acutely dissociated D1+ and D1− cells as shown in *A*. *C*, normalized GFP and GlyR α1 immunofluorescence in dissociated neurons. Blue line indicates cut-off between cell types at the mean GFP signal. Cross-bars indicate mean ± SEM for D1+ and D1− cells. Intensity was measured at an optical section at the cell centre ($n = 14$ and $n = 19$, respectively, GlyR *vs.* GlyR $^*P < 0.05$, GFP *vs.* GFP $^{***} < 0.001$, unpaired Student's *t* test).

PCR detected the preferential expression of GlyR in mouse nAc at a moderate expression level between the low expression found in HC and the high levels in BS and SC. Furthermore, using HA-tagged ribosomes from nAc of D1 and D2-Cre-RiboTag mice, we found ribosome-associated transcripts for α1 and β subunits enriched in both MSNs (α1 Input = 1.00 ± 0.188; DRD1 = 4.47 ± 0.98, $P = 0.018$; DRD2 = 3.83 ± 0.035, $P = 0.035$; β Input = 1.00 ± 0.106; DRD1 = 2.59 ± 0.531, $P = 0.045$; DRD2 = 3.12 ± 0.223, $P = 0.0001$; Fig. 3*A* and *C*), while α2 was enriched in DRD1 MSNs but reduced in DR2D MSNs (α1 Input = 1.00 ± 0.084; DRD1 = 1.31 ± 0.096, $P = 0.052$; DRD2 = 0.68 ± 0.076, $P = 0.024$; Fig. 3*B*).

To follow up with the characterization of GlyR subunits at the mRNA level, we used IHC analysis of DRD1-GFP mouse brain sections to validate protein expression of α1 subunits in GFP-expressing D1+ MSNs. Utilizing the subunit-specific mAb2b monoclonal mouse antibody (Wassle *et al.* 1998), we detected the expression of GlyR α1 (red signal) in the core and shell regions of the nAc (Fig. 4*A* and *B*). The level of GlyR staining was variable between the neurons and it was found in the soma and in the periphery of D1+ MSNs and D1− MSNs, suggesting membrane localization (Fig. 4*C*). Moreover, the same analysis done in acutely dissociated accumbal neurons revealed that GlyR α1 was more strongly expressed in D1+ than in D1− MSNs (Fig. 5*A*–*C*). Figure 5*B* shows a maximum intensity projection of the single fluorescent channel for the GlyR α1 signal in D1+ and D1− MSNs ($z = 16$, 7.23 μm). The quantified α1 signal of a single optical section at the centre of the cell soma is shown in Fig. 5*C* (D1+ 17 ± 2% *vs.* D1− 12 ± 1% of maximum pixel intensity, $n = 14$ D1+ MSNs and $n = 19$ D1− MSNs, $^*P = 0.0104$). The data show that both cell types express α1 GlyR subunits and are in agreement with the previous data on ribosome-associated transcripts for α1 (Fig. 3).

To address whether different GlyR subunits can be expressed in a single neuron, brain sections of nAc were co-stained using a polyclonal GlyR pan-α antibody that binds to all α subunits (Fig. 6*A*) and an antibody for GlyR β (Fig. 6*B*), DAPI and anti-GFP antibody (not shown). This co-staining showed the presence of α and β subunits in single accumbal D1+ and D1− MSNs. In addition, the staining showed some degree of co-localization between GlyR α and GlyR β (Fig. 6*A* and *B*, arrowheads), suggesting

the existence of heteromeric receptors, as well as GlyR α that did not co-localize with GlyR β (Fig. 6*A* and *B*, arrows), suggesting the presence of homomeric receptors. Similar to GlyR α1 findings (Fig. 4), co-staining of pan-α and β also featured a punctated signal found mainly in the cell periphery (Fig. 6*A* and *B*).

To investigate the α subunits expressed in D1+ and D1− MSNs of the nAc, we performed IHC in accumbal brain sections using the pan-α antibody (Fig. 6*C*) and the GlyR α1-specific mAb2b (Fig. 6*D*) with DAPI and anti-GFP antibody (not shown), which showed labelling of the pan-α antibody and α1 in both cell types. Signal intensity of the pan-α labelling was augmented to facilitate comparison with α1. While the GlyR α1 signal co-localized with the pan-α staining (Fig. 6*C* and *D*, arrowheads), as expected in the presence of GlyR α1, the same cells also presented pan-α signal that was not co-localized with α1 (Fig. 6*C* and *D*, arrows) in both D1+ and D1− MSNs, indicating the presence of other GlyR α subunits besides α1. Thus, IHC confirmed co-expression of GlyR β and α subunits, as well as GlyR α1 and other α subunits in accumbal D1+ MSNs.

Accumbal MSNs express glycine-mediated currents sensitive to ethanol

After learning that MSNs express α1 and α2 subunits, and that non-D1+ MSNs express lower levels of α2, we decided

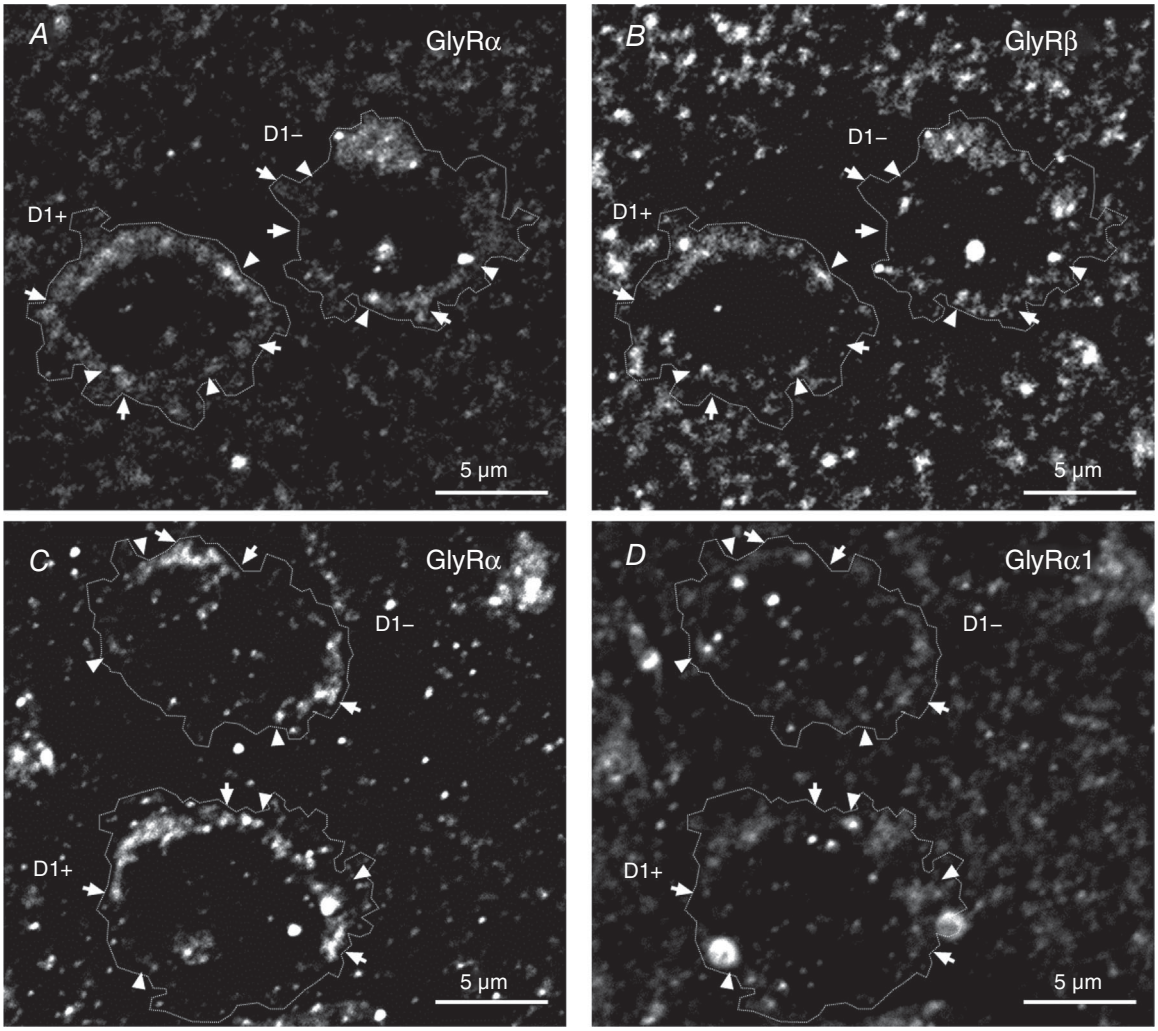

Figure 6. Presence of GlyR α and β subunits in D1+ and D1− MSNs of nAc brain sections
A and *B*, immunohistochemistry of GlyR pan-α (*A*) and GlyR β (*B*) shows that some clusters of GlyR α co-localized with or are in close apposition to GlyR β (arrowheads) in D1+ and D1− cells in mouse brain sections of nAc (GFP and DAPI signal not shown). Some clusters were also found without presenting this co-localization pattern (arrows). *C* and *D*, immunohistochemistry of GlyR pan-α (*C*) and GlyR α1 (*D*) in mouse brain sections of nAc. The image shows co-localization and apposition of GlyR α1 and pan-α (arrowheads) and other pan-α signals not co-localized with α1 signal (arrows) in D1+ and D1− cells (GFP and DAPI signal not shown). Channel intensity of GlyR pan-α was adjusted to be comparable to GlyR β and α1, respectively.

to investigate the presence of glycine-activated currents using whole-cell patch clamp in acutely dissociated accumbal neurons and brain slices. Data show that D1+ and D1− MSNs had glycine-activated currents (Fig. 7*A*). The currents had different properties in the two cell types. For instance, the shape of the current trace in D1− MSNs indicated a smaller level of desensitization. Also, the curves of response–glycine concentrations in D1− MSNs were slightly displaced to the right. For instance, the value for EC_{50} was 38 ± 4 μM ($n = 14$) in D1+ and 61 ± 22 μM ($n = 10$) in D1− MSNs (Fig. 7*B*). These data are consistent with the presence of predominantly α1 subunits (Yevenes *et al.* 2006). In agreement with the higher GlyR α1 immunofluorescence detected in D1+ MSNs (Fig. 5), whole-cell recordings in D1+ MSNs revealed higher amplitude glycine-induced currents (Fig. 7*A*) and current density than in D1− (D1+: 22 ± 5 pA pF^{-1}, $n = 6$; D1−: 7 ± 1 pA pF^{-1}, $n = 21$, $^{***}P < 0.001$; Fig. 7*C*). In both cases, the currents were completely and reversibly blocked by 1 μM strychnine (STN) (Fig. 7*D*).

After showing that D1+ and D1− MSNs present glycine-activated currents, we examined the sensitivity of these currents to ethanol and found that the glycine-evoked currents were equally potentiated by 100 mM in both cell types (Fig. 8*A* and *B*). In addition to examining ethanol effects on dissociated neurons, we also tested its effects on a glycine-activated tonic current recorded in brain slices (Fig. 9). This tonic current was studied under conditions that pharmacologically blocked $GABA_A$- AMPA- and NMDA-evoked currents with a cocktail of bicuculline (10 μM), CNQX (10 μM) and D-APV (50 μM) applied to nAc slices. The data show that application of 10 μM Org24598, an inhibitor of the GlyT1, caused an inward current shift of −21 ± 5 pA that was reversed by 1 μM of strychnine (STN), leading to a positive shift of 11 ± 5 pA from the control condition ($n = 5$, $^{**}P < 0.01$; Fig. 9*A*–*C*). The amplitude of this tonic current was also increased by the application of 100 mM ethanol, resulting in an inward current shift of −6 ± 2 pA that was blocked by 1 μM STN (Fig. 9*D*–*F*).

To determine a possible effect on the excitability of MSNs resulting from the ethanol-mediated potentiation of GlyRs, action potentials (APs) were recorded in D1+ MSNs in nAc slices using the current-clamp configuration. The number and frequency of APs elicited from a holding potential of −68 ± 1 mV were significantly decreased ($^{*}P < 0.05$) by −42 ± 24% after application of 100 mM ethanol, while the inhibitory effects of ethanol were blocked by co-application of STN (−14 ± 23%), and AP frequency increased to +29 ± 15% ($^{*}P < 0.05$) in the presence of 1 μM STN without ethanol ($n = 7$; Fig. 10*A* and *B*). Thus, electrophysiological recordings confirm the functionality of GlyRs, with glycine and ethanol responses of D1+ and D1− cells.

Discussion

This study showed the presence of GlyR α1, α2, α3 and GlyR β in D1+ and D1− MSNs from mouse nAc. We also show that both cell populations have ethanol-sensitive

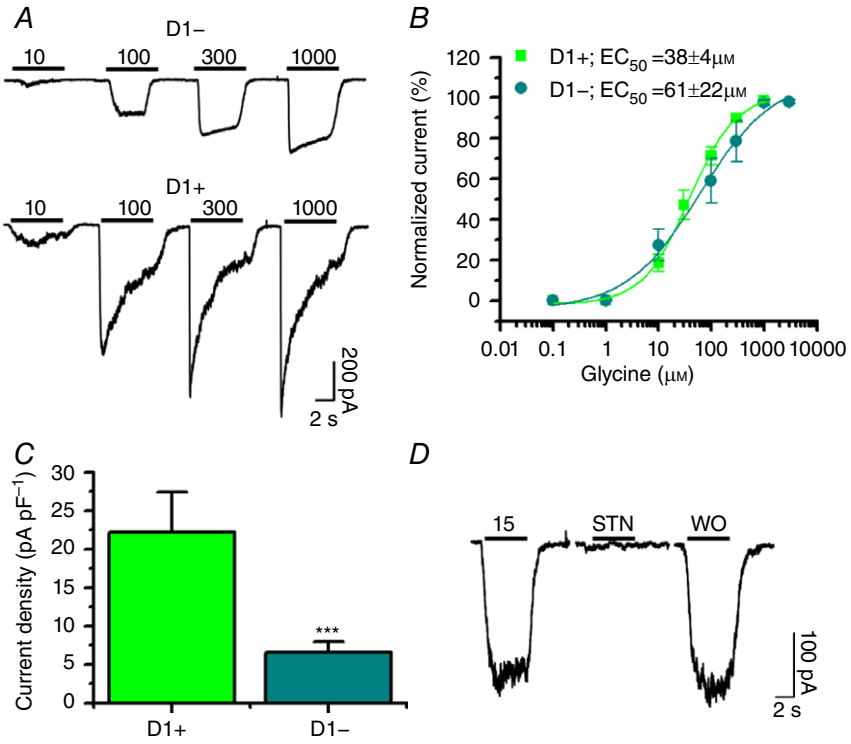

Figure 7. Glycine-activated currents in dissociated D1+ and D1−MSN from nAc
A, representative responses to 10, 100, 300 and 1000 μM glycine in D1+ and D1− MSNs. Lower traces were recorded with 15 μM glycine, 15 μM glycine plus 1 μM STN and washout (WO) in a D1+ MSN. *B*, glycine concentration–response curve (0.1–3000 μM) of D1+ (green squares) and D1− (cyan circles). The curve was normalized to the maximum response ($n = 14$ and $n = 10$ for D1+ and D1−, respectively). *C*, current density indicates significantly lower current density in D1− MSNs ($n = 6$ and $n = 21$, respectively, mean ± SEM. $^{***}P < 0.001$). *D*, traces showing the complete inhibition of the glycine current with application of 1 μM STN.

glycinergic currents. D1+ MSNs exhibited a stronger GlyR α1 signal detected by immunofluorescence, as well as an almost 40% lower EC_{50} in glycine-evoked currents. Furthermore, patch clamp recordings confirmed an effect of ethanol on the glycine-activated current and on MSN excitability. The present results suggest that the ethanol-sensitive GlyR subunits might play an important role in addiction behaviour by controlling the excitability and output of this region.

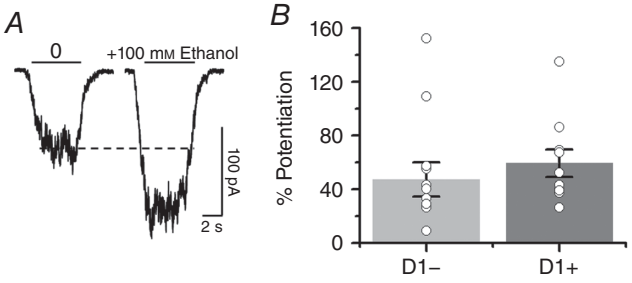

Figure 8. Glycine currents evoked in dissociated MSNs are sensitive to ethanol
A, traces of glycine-evoked currents were obtained in a D1+ MSN in the absence and presence of ethanol at EC_{10} concentrations of glycine. *B*, bar graph showing the potentiating effect of 100 mM ethanol on the peak amplitude of the glycine-activated current in D1+ and D1− MSNs ($n = 10$ and $n = 13$, respectively, mean ± SEM).

Presence of GlyR subunits in nAc

In the present study, using qPCR, we detected the expression of α1, α2, α3 and β subunits in the mouse nAc. Interestingly, our data showed a similar trend to that found in the rat, although α1 was expressed to a greater extent than α2 in the mouse nAc (Sato *et al.* 1991, 1992; Racca *et al.* 1998; Jonsson *et al.* 2012). This finding highlights the need for caution when comparing different model systems even in closely related species, as exemplified by the differing effect of ethanol on $GABA_AR$ (Forstera *et al.* 2016). As expected, nAc showed lower expression of GlyRs than in BS and SC (about 30-fold).

It is interesting to note that while conventional PCR indicated the predominant expression of the GlyR α1ins and α2A, both splice variants of all subunits were expressed (Fig. 2*A*), including the mouse-specific alternative GlyR β splice variant of unknown function recently described in mouse SC (Winkelmann *et al.* 2015). These results open the possibility for expression of splice-specific GlyR function in the mouse nAc, as recently described for GlyR α1ins and GlyR α3K (Eichler *et al.* 2009; Legendre *et al.* 2009; Forstera *et al.* 2014; Meier *et al.* 2014). Although low, the expression of GlyR α3 might nevertheless play a role in the pre-synaptic regulation of synaptic transmission in the mesolimbic network. It was previously reported that even a small population of RNA-edited high affinity

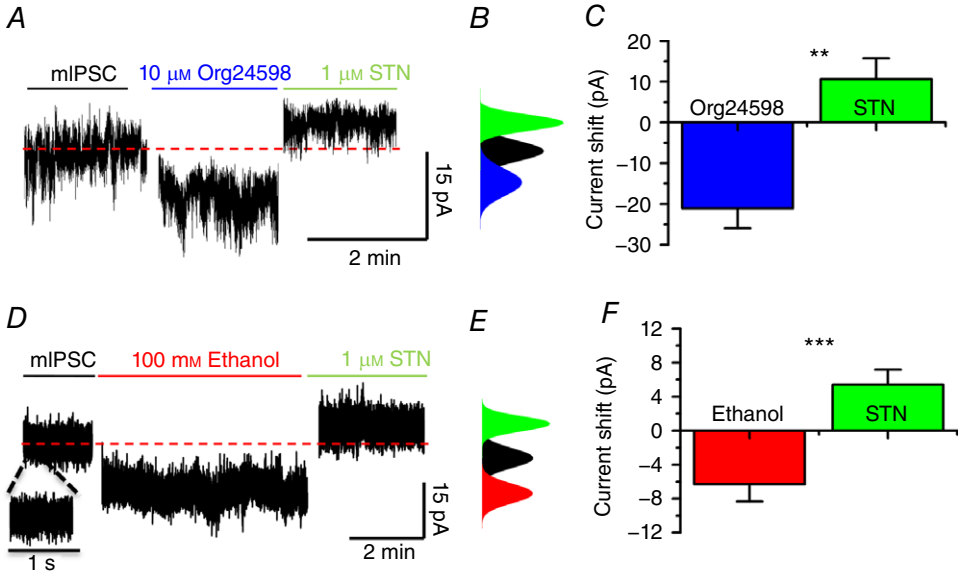

Figure 9. Potentiation of GlyR-mediated tonic current by ethanol in MSNs
A and *B*, traces showing recording of tonic current in a D1+ MSN and the associated current shift of the all-points histogram demonstrating the inward current shift in the presence of 10 μM Org24598 (blue) and a positive shift in the current after application of 1 μM STN (green). *C*, bar chart showing the change in amplitude of tonic current after application of Org24598 and STN (mean ± SEM, $n = 5$, one-way ANOVA $^{**}P < 0.01$). *D* and *E*, representative current trace and the all-points histogram for the holding current in the presence of 100 mM ethanol (red) and 1 μM STN (green). The expanded current trace in *D* shows no appreciable synaptic currents. *F*, bar chart showing the changes in the amplitude of the tonic current in the presence of ethanol and STN on tonic current (mean ± SEM, $n = 11$, one-way ANOVA $^{***}P < 0.001$).

GlyRs might have a strong physiological impact (Meier *et al.* 2005, 2014; Eichler *et al.* 2008; Legendre *et al.* 2009). It is unlikely, however, that α2 and α3 homopentamer GlyRs might play a major role in the effects of ethanol in the nAc, because GlyRs consisting of these subunits have been shown to exhibit low sensitivity to modulation by ethanol (Aguayo *et al.* 2014; Sanchez *et al.* 2015; Burgos *et al.* 2015*b*). Accordingly, the altered sensitivity to ethanol reported in GlyR α3 knock-out mice might be affected by global compensation rather than a direct action of ethanol on this subunit (Blednov *et al.* 2015).

The expression of GlyRs at the cellular level was confirmed by IHC and ICC, showing the presence of GlyR α and β, similar to previous findings in the rat nAc (Jonsson *et al.* 2012; Weltzien *et al.* 2012). While GlyRs were detected previously in accumbal neurons (Jonsson *et al.* 2012; Weltzien *et al.* 2012), in this study we confirmed the presence of the highly ethanol-sensitive GlyR α1 subunit in the mouse nAc with a higher functional expression in D1+ MSNs compared to D1− cells, raising particular interest for D1+ MSNs in relation to ethanol-induced effects on the feedback loop between nAc and VTA (Koob & Nestler, 1997). A higher GlyR α1 level was detected in D1+ than in D1−MSNs, indicating different contributions of α1 GlyRs to inhibition in these cell populations. The data are consistent with D1+ MSNs expressing predominantly α1 subunits, which have an EC_{50} value of about 40 μM, lower than α2 and α3 subunits (Yevenes *et al.* 2006). Also, the analysis of HA-tagged ribosomes from nAc of D1 and D2-Cre-RiboTag mice confirmed transcripts for α1, α2 and β subunits. Interestingly, D1 and D2 MSNs showed higher levels of α1 and β than α2 subunits.

Presence of ethanol-sensitive GlyRs in the CNS

GlyRs provide a critical level of neuronal inhibition in the BS and SC. GlyRs have been shown to be sensitive to potentiation by ethanol, resulting in a concentration-dependent and reversible increase in apparent agonist affinity in the SC and more recently in several regions of the CNS (Aguayo *et al.* 1994; Lu & Ye, 2011; Maguire *et al.* 2014; Salling & Harrison, 2014). Previous data showed that the potentiation of GlyRs started at an ethanol concentration of 10 mM and that it increased up to a concentration of 100 mM. The potentiation of the GlyR by ethanol is affected by the interaction of the α1 subunit's large intracellular loop with G$\beta\gamma$ and this interaction was recently shown to contribute to the acute motor and sedative effects of ethanol (Yevenes *et al.* 2010; Aguayo *et al.* 2014). Although the structure of the intracellular loop is still not resolved, the existence of alpha helix was proposed (Burgos *et al.* 2015*a*). These regions should play a role on the protein–protein interaction with G$\beta\gamma$ and potentially for therapeutic development (San Martin *et al.* 2016).

It was previously reported that the ability of ethanol to potentiate GlyRs depends on the subunit composition of the receptor (Yevenes *et al.* 2006). For example, while an ethanol-sensitive GlyR α1 subunit is amply found in BS and SC, GlyRs found in the upper brain regions are thought to be constituted mostly of the less sensitive GlyR α2 and α3 subunits, which are little affected by ethanol (Aguayo *et al.* 2004; Yevenes *et al.* 2008, 2010). Based on these previous studies, we can conclude that the potentiation of GlyR function induced by ethanol in nAc neurons is probably due to the presence of α1 subunits, which is consistent with the present subunit expression data. Therefore, in terms of the present results, the presence of α1 subunits in nAc is likely to play a role in the function of the mesolimbic circuitry, including addictive behaviours.

It is believed that most of the GlyRs expressed in supra-tentorial regions of the CNS are non-synaptic, and accordingly they may participate in the mediation of tonic inhibition (Avila *et al.* 2013). In agreement, using

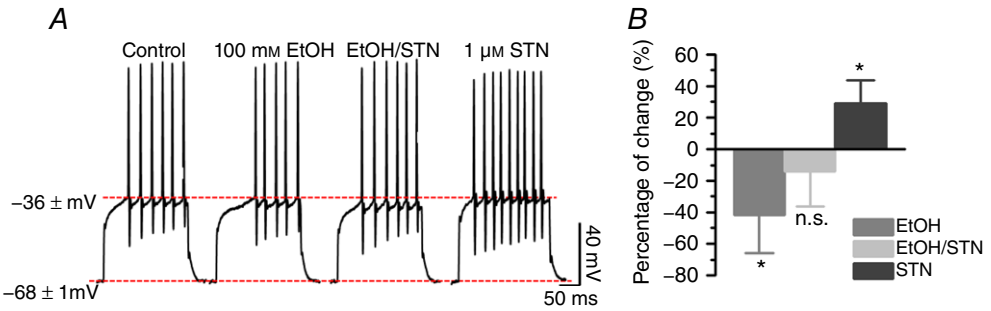

Figure 10. Ethanol decreased action potential firing in MSNs
A, voltage traces showing the inhibitory effect of ethanol (100 mM) on AP frequency. The inhibitory effect of ethanol was reversed by co-application of 1 μM STN. The effect of STN alone was excitatory supporting the inhibitory role of GlyRs. *B*, the percentage change in AP frequency elicited by a 225 pA current pulse in the presence of ethanol alone or with STN (mean ± SEM, $n = 7$, one-way ANOVA, $^*P < 0.05$). [Colour figure can be viewed at wileyonlinelibrary.com]

brain slices we found that application of either ethanol or the GlyT1-specific antagonist Org24598 affected the STN-sensitive tonic current in D1+ MSNs. It can therefore be concluded that this current is probably primarily mediated by GlyR α1 subunits. In addition, the excitability of these neurons was likewise reduced in the presence of ethanol in an STN-sensitive manner, as indicated by the decrease in AP frequency induced by depolarizing current application, thus attesting to a physiological impact of ethanol on the excitability of D1+ MSNs. The effect of ethanol on the holding tonic current was not associated with changes on transient miniature IPSCs since the frequency of minis is low (0.27 $\pm$ 0.1 Hz, $n = 5$) in the presence of TTX and receptor blockers (see Methods).

Ethanol sensitivity of GlyR in accumbal MSNs

The present study shows the presence of GlyR α1 in accumbal MSNs and indicates that these receptors provide a tonic inhibition level activating a sustained current that is sensitive to ethanol. Using PCR, RiboTag and immunochemistry techniques, we were able to confirm the expression of GlyR α1, α2, α3 and β in accumbal neurons, and electrophysiological recordings demonstrated that D1+ and D1− MSNs express ethanol-sensitive glycinergic currents. There were some differences in the properties of the glycine current in these two cell types. For example, D1+ MSNs exhibited greater α1 immunoreactivity together with a higher current density, indicating higher expression of this subunit. Also, we found that the EC_{50} for activation in D1+ MSNs was lower than in D1−, suggesting differences in subunit expression, with α1 being expressed predominantly in D1+ MSNs. Because the mean channel conductance for the GlyR in MSNs, recorded with outside out recordings under isomolar concentration of Cl^-, was approximately 40 pS at a holding potential of −60 mV (not shown), the presence of heteromeric GlyR α1/β in the nAc can be inferred (Yevenes *et al.* 2010; Avila *et al.* 2013). The potentiating effect could be attributed to an increase in the single channel opening probability, but not of the mean conductance, in the presence of ethanol. Furthermore, AP recording from D1+ MSNs confirmed a suppressing effect of ethanol on the excitability of these neurons, an effect that was mediated by an STN-sensitive component.

Proposed role of GlyRs on mesolimbic physiology

It was previously reported that the application of a GlyR agonist to the nAc resulted in an increase in dopamine, an effect that was inhibited by STN, while GlyRs in the VTA had the inverse effect (Molander & Soderpalm, 2005*b*; Soderpalm *et al.* 2009; Jonsson *et al.* 2014). The present study shows that ethanol reduces the excitability of D1+ MSNs by GlyR potentiation. Thus, it is possible that GlyR potentiation in the nAc plays a role in the increase in accumbal dopamine, by a negative and indirect pathway, following ethanol consumption (Molander *et al.* 2005; Molander & Soderpalm, 2005*a*, *b*; Spanagel, 2009; Jonsson *et al.* 2014, 2017; Clarke *et al.* 2015). Finally, the presence of GlyRs in D1 MSN (Kravitz & Kreitzer, 2012) suggests an important role of these receptors in the activation of the direct pathway between VTA and nAc (Koob & Nestler, 1997), possibly by neuronal disinhibition. The present data, together with a recent study that showed that a small molecule can reduce the sedative effects of ethanol (San Martin *et al.* 2016) by interfering with the GlyR-G$\beta\gamma$ protein/protein interaction, support the notion that the present type of study can lead to the development of therapeutics to treat toxic and addictive ethanol behaviours.

References

Aguayo LG, Castro P, Mariqueo T, Munoz B, Xiong W, Zhang L, Lovinger DM & Homanics GE (2014). Altered sedative effects of ethanol in mice with α1 glycine receptor subunits that are insensitive to G$\beta\gamma$ modulation. *Neuropsychopharmacology* **39**, 2538–2548.

Aguayo LG, Pancetti FC, Klein RL & Harris RA (1994). Differential effects of GABAergic ligands in mouse and rat hippocampal neurons. *Brain Res* **647**, 97–105.

Aguayo LG, van Zundert B, Tapia JC, Carrasco MA & Alvarez FJ (2004). Changes on the properties of glycine receptors during neuronal development. *Brain Res Rev* **47**, 33–45.

Avila A, Nguyen L & Rigo JM (2013). Glycine receptors and brain development. *Front Cell Neurosci* **7**, 184.

Bell DS (1973). The experimental reproduction of amphetamine psychosis. *Arch Gen Psychiatry* **29**, 35–40.

Blednov YA, Benavidez JM, Black M, Leiter CR, Osterndorff-Kahanek E & Harris RA (2015). Glycine receptors containing α2 or α3 subunits regulate specific ethanol-mediated behaviors. *J Pharmacol Exp Ther* **353**, 181–191.

Burgos CF, Castro PA, Mariqueo T, Bunster M, Guzman L & Aguayo LG (2015*a*). Evidence for α-helices in the large intracellular domain mediating modulation of the α1-glycine receptor by ethanol and G$\beta\gamma$. *J Pharmacol Exp Ther* **352**, 148–155.

Burgos CF, Munoz B, Guzman L & Aguayo LG (2015*b*). Ethanol effects on glycinergic transmission: from molecular pharmacology to behavior responses. *Pharmacol Res* **101**, 18–29.

Burgos CF, Yevenes GE & Aguayo LG (2016). Structure and pharmacologic modulation of inhibitory glycine receptors. *Mol Pharmacol* **90**, 318–325.

Carlsson A & Lindqvist M (1963). Effect of chlorpromazine or haloperidol on formation of 3methoxytyramine and normetanephrine in mouse brain. *Acta Pharmacol Toxicol* **20**, 140–144.

Chandra R, Francis TC, Konkalmatt P, Amgalan A, Gancarz AM, Dietz DM & Lobo MK (2015). Opposing role for Egr3 in nucleus accumbens cell subtypes in cocaine action. *J Neurosci* **35**, 7927–7937.

Clarke RB, Soderpalm B, Lotfi A, Ericson M & Adermark L (2015). Involvement of inhibitory receptors in modulating dopamine signaling and synaptic activity following acute ethanol exposure in striatal subregions. *Alcohol Clin Exp Res* **39**, 2364–2374.

Di Chiara G (2000). Role of dopamine in the behavioural actions of nicotine related to addiction. *Eur J Pharmacol* **393**, 295–314.

Eichler SA, Förstera B, Smolinsky B, Juttner R, Lehmann TN, Fahling M, Schwarz G, Legendre P & Meier JC (2009). Splice-specific roles of glycine receptor α 3 in the hippocampus. *Eur J Neurosci* **30**, 1077–1091.

Eichler SA, Kirischuk S, Jüttner R, Schäfermeier PK, Legendre P, Lehmann TN, Gloveli T, Grantyn R & Meier JC (2008). Glycinergic tonic inhibition of hippocampal neurons with depolarising GABAergic transmission elicits histopathological signs of temporal lobe epilepsy. *J Cell Mol Med* **12**, 2848–2866.

Forstera B, Dildar a Dzaye O, Winkelmann A, Semtner M, Benedetti B, Markovic DS, Synowitz M, Wend P, Fahling M, Junier MP, Glass R, Kettenmann H & Meier JC (2014). Intracellular glycine receptor function facilitates glioma formation *in vivo*. *J Cell Sci* **127**, 3687–3698.

Förstera B, Belaidi AA, Jüttner R, Bernert C, Tsokos M, Lehmann TN, Horn P, Dehnicke C, Schwarz G & Meier JC (2010). Irregular RNA splicing curtails postsynaptic gephyrin in the cornu ammonis of patients with epilepsy. *Brain* **133**, 3778–3794.

Forstera B, Castro PA, Moraga-Cid G & Aguayo LG (2016). Potentiation of gamma aminobutyric acid receptors ($GABA_AR$) by ethanol: how are inhibitory receptors affected? *Front Cell Neurosci* **10**, 114.

Froh M, Thurman RG & Wheeler MD (2002). Molecular evidence for a glycine-gated chloride channel in macrophages and leukocytes. *Am J Physiol Gastrointest Liver Physiol* **283**, G856–G863.

Guzman L, Moraga-Cid G, Avila A, Figueroa M, Yevenes GE, Fuentealba J & Aguayo LG (2009). Blockade of ethanol-induced potentiation of glycine receptors by a peptide that interferes with G$\beta\gamma$ binding. *J Pharmacol Exp Ther* **331**, 933–939.

Husson Z, Rousseau CV, Broll I, Zeilhofer HU & Dieudonne S (2014). Differential GABAergic and glycinergic inputs of inhibitory interneurons and Purkinje cells to principal cells of the cerebellar nuclei. *J Neurosci* **34**, 9418–9431.

Jeanes ZM, Buske TR & Morrisett RA (2011). *In vivo* chronic intermittent ethanol exposure reverses the polarity of synaptic plasticity in the nucleus accumbens shell. *J Pharmacol Exp Ther* **336**, 155–164.

Jonsson S, Adermark L, Ericson M & Soderpalm B (2014). The involvement of accumbal glycine receptors in the dopamine-elevating effects of addictive drugs. *Neuropharmacology* **82**, 69–75.

Jonsson S, Morud J, Pickering C, Adermark L, Ericson M & Soderpalm B (2012). Changes in glycine receptor subunit expression in forebrain regions of the Wistar rat over development. *Brain Res* **1446**, 12–21.

Jonsson S, Morud J, Stomberg R, Ericson M & Soderpalm B (2017). Involvement of lateral septum in alcohol's dopamine-elevating effect in the rat. *Addict Biol* **22**, 93–102.

Koob GF (1998). Circuits, drugs, and drug addiction. *Adv Pharmacol* **42**, 978–982.

Koob GF & Nestler EJ (1997). The neurobiology of drug addiction. *J Neuropsychiatry Clin Neurosci* **9**, 482–497.

Kravitz AV & Kreitzer AC (2012). Striatal mechanisms underlying movement, reinforcement, and punishment. *Physiology* **27**, 167–177.

Kuhse J, Kuryatov A, Maulet Y, Malosio ML, Schmieden V & Betz H (1991). Alternative splicing generates two isoforms of the alpha 2 subunit of the inhibitory glycine receptor. *FEBS Lett* **283**, 73–77.

Legendre P, Förstera B, Jüttner R & Meier JC (2009). Glycine receptors caught between genome and proteome - Functional implications of RNA editing and splicing. *Front Mol Neurosci* **2**, 23.

Li J, Nie H, Bian W, Dave V, Janak PH & Ye JH (2012). Microinjection of glycine into the ventral tegmental area selectively decreases ethanol consumption. *J Pharmacol Exp Ther* **341**, 196–204.

Lu Y & Ye JH (2011). Glycine-activated chloride currents of neurons freshly isolated from the prefrontal cortex of young rats. *Brain Res* **1393**, 17–22.

Lynch JW (2009). Native glycine receptor subtypes and their physiological roles. *Neuropharmacology* **56**, 303–309.

Maguire EP, Mitchell EA, Greig SJ, Corteen N, Balfour DJ, Swinny JD, Lambert JJ & Belelli D (2014). Extrasynaptic glycine receptors of rodent dorsal raphe serotonergic neurons: a sensitive target for ethanol. *Neuropsychopharmacology* **39**, 1232–1244.

Martin G & Siggins GR (2002). Electrophysiological evidence for expression of glycine receptors in freshly isolated neurons from nucleus accumbens. *J Pharmacol Exp Ther* **302**, 1135–1145.

Meier JC, Henneberger C, Melnick I, Racca C, Harvey RJ, Heinemann U, Schmieden V & Grantyn R (2005). RNA editing produces glycine receptor $\alpha 3^{P185L}$ resulting in high agonist potency. *Nat Neurosci* **8**, 736–744.

Meier JC, Semtner M, Winkelmann A & Wolfart J (2014). Presynaptic mechanisms of neuronal plasticity and their role in epilepsy. *Front Cell Neurosci* **8**, 164.

Meredith GE (1999). The synaptic framework for chemical signaling in nucleus accumbens. *Ann N Y Acad Sci* **877**, 140–156.

Molander A, Lido HH, Lof E, Ericson M & Soderpalm B (2007). The glycine reuptake inhibitor Org 25935 decreases ethanol intake and preference in male wistar rats. *Alcohol Alcohol* **42**, 11–18.

Molander A, Lof E, Stomberg R, Ericson M & Soderpalm B (2005). Involvement of accumbal glycine receptors in the regulation of voluntary ethanol intake in the rat. *Alcohol Clin Exp Res* **29**, 38–45.

Molander A & Soderpalm B (2005*a*). Accumbal strychnine-sensitive glycine receptors: an access point for ethanol to the brain reward system. *Alcohol Clin Exp Res* **29**, 27–37.

Molander A & Soderpalm B (2005*b*). Glycine receptors regulate dopamine release in the rat nucleus accumbens. *Alcohol Clin Exp Res* **29**, 17–26.

Pfaffl MW (2001). A new mathematical model for relative quantification in real-time RT-PCR. *Nucleic Acids Res* **29**, e45.

Racca C, Gardiol A & Triller A (1998). Cell-specific dendritic localization of glycine receptor α subunit messenger RNAs. *Neuroscience* **84**, 997–1012.

Renteria R, Maier EY, Buske TR & Morrisett RA (2017). Selective alterations of NMDAR function and plasticity in D1 and D2 medium spiny neurons in the nucleus accumbens shell following chronic intermittent ethanol exposure. *Neuropharmacology* **112**, 164–171.

Salling MC & Harrison NL (2014). Strychnine-sensitive glycine receptors on pyramidal neurons in layers II/III of the mouse prefrontal cortex are tonically activated. *J Neurophysiol* **112**, 1169–1178.

San Martin L, Cerda F, Jin C, Jimenez V, Yevenes GE, Hernandez T, Nova D, Fuentealba J, Aguayo LG & Guzman L (2016). Reversal of ethanol-induced intoxication by a novel modulator of G$\beta\gamma$ protein potentiation of the glycine receptor. *J Biol Chem* **291**, 18791–18798.

Sanchez A, Yevenes GE, San Martin L, Burgos CF, Moraga-Cid G, Harvey RJ & Aguayo LG (2015). Control of ethanol sensitivity of the glycine receptor α3 subunit by transmembrane 2, the intracellular splice cassette and C-terminal domains. *J Pharmacol Exp Ther* **353**, 80–90.

Sato K, Kiyama H & Tohyama M (1992). Regional distribution of cells expressing glycine receptor α2 subunit mRNA in the rat brain. *Brain Res* **590**, 95–108.

Sato K, Zhang JH, Saika T, Sato M, Tada K & Tohyama M (1991). Localization of glycine receptor α1 subunit mRNA-containing neurons in the rat brain: an analysis using *in situ* hybridization histochemistry. *Neuroscience* **43**, 381–395.

Snyder SH (1973). Amphetamine psychosis: a "model" schizophrenia mediated by catecholamines. *Am J Psychiatry* **130**, 61–67.

Soderpalm B, Lof E & Ericson M (2009). Mechanistic studies of ethanol's interaction with the mesolimbic dopamine reward system. *Pharmacopsychiatry* **42**(Suppl 1), S87–94.

Spanagel R (2009). Alcoholism: a systems approach from molecular physiology to addictive behavior. *Physiol Rev* **89**, 649–705.

Stanic K, Montecinos H & Caprile T (2010). Subdivisions of chick diencephalic roof plate: implication in the formation of the posterior commissure. *Dev Dyn* **239**, 2584–2593.

Volkow ND & Li TK (2004). Drug addiction: the neurobiology of behaviour gone awry. *Nature Rev Neurosci* **5**, 963–970.

Wassle H, Koulen P, Brandstatter JH, Fletcher EL & Becker CM (1998). Glycine and GABA receptors in the mammalian retina. *Vision Res* **38**, 1411–1430.

Weltzien F, Puller C, O'Sullivan GA, Paarmann I & Betz H (2012). Distribution of the glycine receptor β-subunit in the mouse CNS as revealed by a novel monoclonal antibody. *J Comp Neurol* **520**, 3962–3981.

Winkelmann A, You X, Grunewald N, Haussler U, Krestel H, Haas CA, Schwarz G, Chen W & Meier JC (2015). Identification of a new genomic hot spot of evolutionary diversification of protein function. *PloS ONE* **10**, e0125413.

Ye JH, Tao L, Ren J, Schaefer R, Krnjevic K, Liu PL, Schiller DA & McArdle JJ (2001). Ethanol potentiation of glycine-induced responses in dissociated neurons of rat ventral tegmental area. *J Pharmacol Exp Ther* **296**, 77–83.

Yevenes GE, Moraga-Cid G, Avila A, Guzman L, Figueroa M, Peoples RW & Aguayo LG (2010). Molecular requirements for ethanol differential allosteric modulation of glycine receptors based on selective G$\beta\gamma$ modulation. *J Biol Chem* **285**, 30203–30213.

Yevenes GE, Moraga-Cid G, Guzman L, Haeger S, Oliveira L, Olate J, Schmalzing G & Aguayo LG (2006). Molecular determinants for G protein $\beta\gamma$ modulation of ionotropic glycine receptors. *J Biol Chem* **281**, 39300–39307.

Yevenes GE, Moraga-Cid G, Peoples RW, Schmalzing G & Aguayo LG (2008). A selective G $\beta\gamma$-linked intracellular mechanism for modulation of a ligand-gated ion channel by ethanol. *Proc Natl Acad Sci USA* **105**, 20523–20528.

Additional information

Competing interests

The authors declare that no competing interests exist.

Author contributions

PCR, ICC, IHC and electrophysiological experiments, and sample collection for IHC were performed in the Laboratory of Neurophysiology, and images were acquired at the CMA core-facility for advanced microscopy at the University of Concepcion. Cell type-specific PCR was performed in the Department of Anatomy and Neurobiology at the University of Maryland School of Medicine. BF, BM and RC planned and performed all experiments, collected and analysed all data and prepared all figures. BF, BM, MKL, RC, DML and LGA contributed to conception and design of the study, interpretation of results, drafting and final version of the manuscript and final revision and editing. All authors reviewed and approved the final manuscript and agree to be accountable for all aspects of the work in ensuring that questions related to the accuracy and integrity of any part of the work are appropriately investigated and resolved. All persons designated as authors qualify for authorship, and all those who qualify for authorship are listed.

Funding

This work was supported in part by Conicyt DPI20140008 (LGA), Conicyt Postdoctoral Grant Fondecyt-3140194 (BF) and Conicyt Grant DPI20140008 (BM).

Acknowledgements

The authors thank Karen Stanic for crucial support and advice with IHC experiments, Jochen C. Meier for fruitful discussion, helpful suggestions and crucial advice, Russel Hodge for language editing and Lauren Aguayo for proofreading of the manuscript, Richard Lowry for providing free use of VassarStats (http://vassarstats.net/index.html), and the Allen Institute for Brain Science for providing free use of the Allen Brain Atlas (http://www.brain-map.org/).

Authors' translational perspective

Neuronal excitability in the mesolimbic system plays a vital role in drug-seeking behaviour and addiction (Spanagel, 2009), and glycine receptors (GlyRs) appear to be involved in the regulation of dopamine levels in the nucleus accumbens (nAc) and ventral tegmental area (VTA) following administration of ethanol and other drugs of abuse. Therefore, we characterized the presence of GlyRs in dopamine receptor D1-positive (D1+) and negative (D1−) neurons. We found that both cell types express ethanol-sensitive GlyR α1 and other subunits, and D1+ neurons were sensitive to ethanol reducing excitability by potentiating tonic currents. We believe that targeting the protein–protein interaction existing between G$\beta\gamma$ and GlyRs (Guzman *et al.* 2009; Burgos *et al.* 2016) might facilitate development of novel therapeutic options to treat abuse of alcohol and other substances (Jonsson *et al.* 2014). In this manner, we expect to reduce the rewarding experience involving the dopaminergic system (Carlsson & Lindqvist, 1963; Bell, 1973; Snyder, 1973). Furthermore, the balance of ethanol-sensitive and -insensitive GlyRs could play a role in the brain's dynamic adaptation to repeated alcohol exposure.